PROCEEDINGS of the
23rd International Congress on Acoustics

9 to 13 September 2019 in Aachen, Germany

Vibration damping capabilities of treatments with frequency and temperature dependent viscoelastic material properties

M. GRÖHLICH[1]; M. BÖSWALD[2]; R. WINTER[3]

[1,2,3] German Aerospace Center (DLR)

Institute of Aeroelasticity, Department for Structural Dynamics and System Identification

Bunsenstraße 10, D-37073 Göttingen, Germany

ABSTRACT

Due to their low mass and stiffening components like frames, stringers and panels, aircraft fuselage structures are prone to vibration. In order to improve acoustic comfort inside a cabin, specific vibration damping of such components would be helpful. Most common damping layouts make use of a viscoelastic material as the main source of vibration energy dissipation. Such material is placed at sensitive positions of a structure to absorb the energy of operational deflection shapes of concern. However, the material behavior of viscoelastic materials varies considerably with frequency and temperature and needs to be considered during the design process. In this paper, a finite element approach for local modelling of viscoelastic damping is presented. A viscoelastic material with frequency and temperature dependent properties is introduced as a dedicated damping material for aeronautic applications. Using the FE method, the consequences of temperature and frequency influence on the vibration damping capability of a Constrained Layer Damping treatment with the particular damping material are presented.

Keywords: Viscoelasticity, Vibration Damping, Damping Layout

1. INTRODUCTION

In the construction of aeronautic structures, lightweight design is essential. Lightweight structures often feature discrete stiffeners as frames and stringers, typically characterized by having both, high stiffness and low mass. As a result of these characteristics, those structures are prone to vibration. In particular, an aircraft fuselage consists of such components, as illustrated in Figure 1.

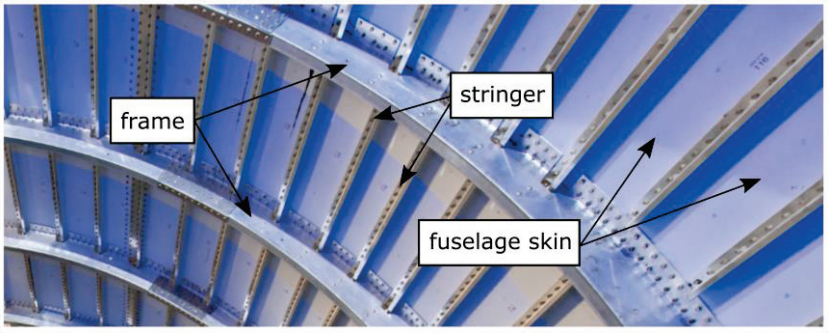

Figure 1 - Fuselage composition of Flight-LAB-demonstrator

Vibrations introduced into the structure are transmitted as structure-borne noise and lead to an increased cabin interior noise due to sound radiation on the fuselage skin. The transmission of structure-borne sound at steady-state excitation, e.g. from turbulent boundary layer or engine induced vibration, can be reduced by increasing damping of the frames. Procedures for an increase of the damping effectiveness include the deliberate generation of shear strain in viscoelastic materials. A common application for vibration damping which utilizes this effect is the Constrained Layer

[1] martin.groehlich@dlr.de
[2] marc.boeswald@dlr.de
[3] rene.winter@dlr.de

Damping treatment (CLD), where a viscoelastic layer is constrained between the stiffer base structure and a stiffer face layer. Since aircraft vibrations cover a wide range of different frequency and temperature ranges during operation, the damping material has to cope with the corresponding influences. Due to the dependence on frequency and temperature of viscoelastic material properties, the damping performance will also vary during operation.

The main objective of this paper is to analyze the effect of frequency and temperature on the damping performance of a viscoelastic material under operating condition. First, the theoretical background of modelling viscoelastic material behavior with respect to frequency and temperature dependence is exemplified. Based on the one-dimensional material model, a transformation into a material model for solid mechanics is presented, allowing for compilation of hysteretic damping matrices for finite element (FE) analysis. Furthermore, a viscoelastic material is introduced and its damping capabilities are analyzed within a CLD treatment for different frequency and temperature levels.

2. THEORETICAL BACKGROUND OF VISCOELASTIC MATERIAL MODELLING

In this section, the basics of idealized viscoelastic material modelling are exemplified. The essential properties are presented and a formulation of the material behavior in frequency domain is provided. Additionally, the temperature dependence on the material behavior is implemented in the material model. By using the finite element method (FEM) it is shown, how viscoelastic material can be incorporated to physically model local viscoelastic damping and to establish a global damping matrix for the structure.

2.1 Linear viscoelasticity in frequency domain

In general, viscoelasticity denotes time dependent material behavior. Under the assumption of a harmonic excitation, a viscoelastic material behavior can be described in terms of a complex modulus, which is a function of the excitation frequency Ω. If constant temperature is assumed, the complex shear modulus G^* can be written as (1):

$$G^*(\Omega) = G'(\Omega) + iG''(\Omega) \tag{1}$$

The real part of the complex notation G' is the storage modulus and denotes the elastic behavior of the material. In contrast to it, the imaginary part G'' is the loss modulus and denotes the viscous or dissipative properties. Both, the real and imaginary part can be expressed by using the parameters of a generalized Maxwell model, often referred to as Prony series. The composition and effects of a generalized Maxwell model are examined in (2-4). The storage modulus can be expressed in terms of the parameters of the generalized Maxwell element:

$$G'(\Omega) = G_0 \left[1 - \sum_{i=1}^{n} \left(\alpha_i - \frac{\alpha_i \tau_{rel,i}^2 \Omega^2}{1 + \tau_{rel,i}^2 \Omega^2} \right) \right], \tag{2}$$

where G_0 is the instantaneous shear modulus at infinitely high frequency, $\tau_{rel,i}$ the relaxation time and α_i the so called relative modulus (5). The equation of the loss modulus is formulated as (5):

$$G''(\Omega) = G_0 \sum_{i=1}^{n} \left(\frac{\alpha_i \tau_{rel,i} \Omega}{1 + \tau_{rel,i}^2 \Omega^2} \right) \tag{3}$$

The ratio of the loss modulus and storage modulus defines the loss factor η:

$$\eta(\Omega) = \frac{G''(\Omega)}{G'(\Omega)} \tag{4}$$

Concerning damping layout, the loss factor is the most important parameter as it quantifies the energy dissipation capability of a material. It is also known as the $\tan\delta$ resulting from dynamic mechanical analysis (DMA).

2.2 Temperature dependence on viscoelastic material properties

The temperature dependence on material properties are taken into account by different shift factors. Various approaches can be found in the literature regarding the shift factor calculation, e.g. in (6).

However, it should be taken into account, that the selection of the approach for the shift factor calculation highly depends on the given material and considered temperature region. In the scope of this paper, the Williams-Landel-Ferry (WLF) as well as the Arrhenius approach are used and briefly presented in the following. For analyzing the material properties' dependence on the temperature, two shifts have to be considered (7):

- Horizontal shift along the frequency axis due to thermal activated rearrangements and higher reaction rate on a molecular level
- Vertical shift along the material property axis due to changes in the type and amount of molecular processes

The frequency shift is defined by a horizontal shift factor ξ_H, resulting from the empirical WLF equation with experimentally determined constants $C1$ and $C2$ relating to a reference temperature T_0 (7):

$$log(\xi_H(T,T_0)) = -\frac{C1 \cdot (T - T_0)}{C2 + T - T_0} \tag{5}$$

The determination of the constants C1 and C2 is based on the evaluation of master curves. Master curves are curve progressions created by merging the measurement data from frequency dependent material characterization at different temperatures.

For the description of the vertical shift, the Arrhenius approach is used. The relation between the experimentally determined activation energy E_A concerning a temperature shift yields the vertical shift factor ξ_V (7):

$$log(\xi_V(T,T_0)) = \frac{0{,}43 \cdot E_A}{R}\left(\frac{1}{T} - \frac{1}{T_0}\right) \tag{6}$$

The parameter R is the universal gas constant. Considering a reference state $S_0(T_0, f_0, G_0', G_0'', \eta_0)$, the corresponding shifted state $S_1(T_1, f_1, G_1', G_1'', \eta_1)$ at an arbitrary temperature T_1 can be determined. If the vertical shift factors for storage and loss modulus are unequal, the shift is calculated by Equations (7) and (8):

$$f_1 = f_0 \cdot \xi_H \tag{7}$$

$$G_1'(f_1) = G_0'(f_0) \cdot \xi_{V,G'} \quad , \quad G_1''(f_1) = G_0''(f_0) \cdot \xi_{V,G''} \quad , \quad \eta_1 = \frac{G_1''}{G_1'} \tag{8}$$

A typical temperature shift of the storage modulus, loss modulus (a) and loss factor (b) of a virtual viscoelastic material, modelled with a generalized Maxwell model, is presented in Figure 2. Therefore, the vertical shift factors for storage and loss modulus are assumed to be equal.

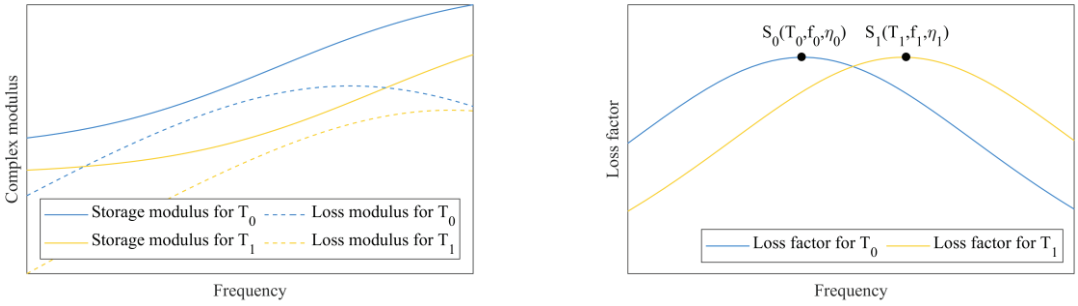

(a) (b)

Figure 2 – Complex modulus (a) and loss factor (b) during a temperature shift

It can be seen in both diagrams that the characteristic evolution of the respective property stays almost the same, but it appears shifted in horizontal and in case of Figure 2(a) also in vertical direction if the temperature changes. In Figure 2(b) the horizontal shift can be clearly observed, since the maximum of the loss factor from the reference state S_0 appears on the same level at higher frequency for a different temperature (S_1). An additional vertical shift for the loss factor would have appeared, if the vertical shift factors of storage and loss modulus had been the same.

2.3 Implementation of viscoelasticity into the finite element method

In order to incorporate viscoelastic material properties into the finite element method, a transformation from the one-dimensional material model into a three-dimensional model is mandatory. Assuming isotropy as an additional material property, the transformation is carried out by Hooke's law. The relationship between stresses $\boldsymbol{\sigma}$ and strains $\boldsymbol{\epsilon}$ is determined by an elasticity matrix $\mathbf{E}$ (8):

$$\boldsymbol{\sigma} = \boldsymbol{E} \cdot \boldsymbol{\epsilon} = \begin{bmatrix} \sigma_{xx} \\ \sigma_{yy} \\ \sigma_{zz} \\ \tau_{xy} \\ \tau_{xz} \\ \tau_{yz} \end{bmatrix} = \frac{E}{(1+\nu)(1-2\nu)} \begin{bmatrix} 1-\nu & \nu & \nu & 0 & 0 & 0 \\ \nu & 1-\nu & \nu & 0 & 0 & 0 \\ \nu & \nu & 1-\nu & 0 & 0 & 0 \\ 0 & 0 & 0 & \frac{1-2\nu}{2} & 0 & 0 \\ 0 & 0 & 0 & 0 & \frac{1-2\nu}{2} & 0 \\ 0 & 0 & 0 & 0 & 0 & \frac{1-2\nu}{2} \end{bmatrix} \cdot \begin{bmatrix} \epsilon_{xx} \\ \epsilon_{yy} \\ \epsilon_{zz} \\ \gamma_{xy} \\ \gamma_{xz} \\ \gamma_{yz} \end{bmatrix} \quad (9)$$

The stress and strain vectors include their corresponding spatial normal parts σ and ϵ, as well as the spatial shear parts τ and γ. Furthermore, the Young's modulus E and the shear modulus G are both related to the Poisson's ratio ν (8):

$$E = 2G(1+\nu) \quad (10)$$

At this point it should be noted, that the elasticity matrix consists of complex entries, as far as viscoelasticity is concerned. In this case, the elasticity matrix $\boldsymbol{E}^*$ can be separated into a real and imaginary part, representing storage and loss behavior, or respectively elasticity and hysteretic damping:

$$\boldsymbol{E}^*(\Omega, T) = \boldsymbol{E}'(\Omega, T) + i\boldsymbol{E}''(\Omega, T) \quad (11)$$

Based on the equivalence of virtual work of external loads with the virtual work of internal stress and strain, a complex element stiffness matrix $\boldsymbol{K}_E^*$ for a finite element can be defined according to the finite element method:

$$\boldsymbol{K}_E^*(\Omega, T) = \int_{V_E} (\boldsymbol{\Theta}\boldsymbol{\varphi}^T)^T \boldsymbol{E}^*(\Omega, T) \boldsymbol{\Theta}\boldsymbol{\varphi}^T dV_E \quad (12)$$

$\boldsymbol{\Theta}$ denotes the differential operator matrix, whereas $\boldsymbol{\varphi}$ conforms to the matrix of element shape functions. Considering the complex notation of Equation (11), the real part of Equation (12) yields a element stiffness matrix $\boldsymbol{K}_E$, whereas the imaginary part yields a hysteretic element damping matrix $\boldsymbol{D}_E$:

$$\boldsymbol{K}_E(\Omega, T) = \int_{V_E} (\boldsymbol{\Theta}\boldsymbol{\varphi}^T)^T \boldsymbol{E}'(\Omega, T) \boldsymbol{\Theta}\boldsymbol{\varphi}^T dV_E \quad (13)$$

$$i\boldsymbol{D}_E(\Omega, T) = i \int_{V_E} (\boldsymbol{\Theta}\boldsymbol{\varphi}^T)^T \boldsymbol{E}''(\Omega, T) \boldsymbol{\Theta}\boldsymbol{\varphi}^T dV_E = i\eta(\Omega, T)\boldsymbol{K}_E(\Omega, T) \quad (14)$$

These element matrices can be used to assemble global system matrices. For example, by using the Boolean matrices $\boldsymbol{B}_E$, elements with viscoelastic material are sorted into global stiffness and hysteretic damping matrices of the whole structure:

$$\boldsymbol{K}(\Omega, T) = \sum_E \boldsymbol{B}_E^T \boldsymbol{K}_E(\Omega, T) \boldsymbol{B}_E \quad (15)$$

$$i\boldsymbol{D}(\Omega, T) = i \sum_E \boldsymbol{B}_E^T \boldsymbol{D}_E(\Omega, T) \boldsymbol{B}_E \quad (16)$$

The sum of the global stiffness and global hysteretic damping matrix forms a global complex stiffness matrix:

$$\boldsymbol{K}^*(\Omega, T) = \boldsymbol{K}(\Omega, T) + i\boldsymbol{D}(\Omega, T) \quad (17)$$

Following this procedure, it is possible to integrate finite elements with frequency and temperature dependent viscoelastic material to represent local dampers in arbitrary structures.

3. INFLUENCE OF FREQUENCY AND TEMPERATURE ON DAMPING

In the following, the influence of frequency and temperature on the damping capability of a viscoelastically damped beam is examined by means of a numerical example.

3.1 Simulation setup

The subject of the analysis is a free-free vibrating, rectangular aluminum beam. According to a CLD treatment a viscoelastic core layer and an aluminum face sheet are applied on the beam, in order to damp occurring vibrations. The corresponding geometric dimensions are shown in Figure 3.

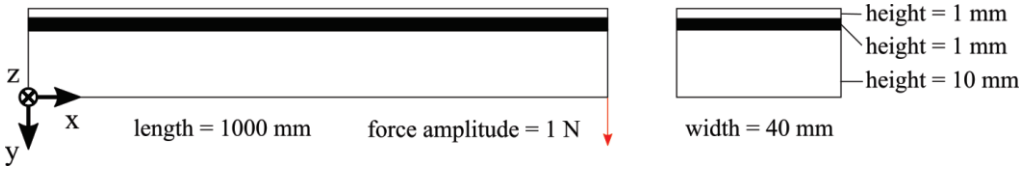

Figure 3 - Geometrical setup of the CLD treatment

The material properties of aluminum are assumed to be isotropic and constant, with a Young's modulus of $E_{Alu} = 7{,}1 \cdot 10^{10}$ Pa and a Poisson's ratio of $\nu_{Alu} = 0{,}33$. Furthermore, the density is $\rho_{Alu} = 2700$ kg/m³ and the structural damping coefficient is chosen to be $\eta_{Alu} = 0{,}005$. For the core layer, the material properties of a particular viscoelastic material are applied. The material is a dedicated mixture of bromobutyl rubber for aeronautic applications as vibration dampers, developed in cooperation with the German Institute of Rubber Technology (Deutsches Institut für Kautschuktechnologie e.V.). The material properties are significantly frequency and temperature dependent and can be characterized by twelve parameter sets of the generalized Maxwell model, as well as by WLF and Arrhenius shifts. In Figure 4, the contour curves of the shear storage modulus and loss factor of bromobutyl rubber are presented.

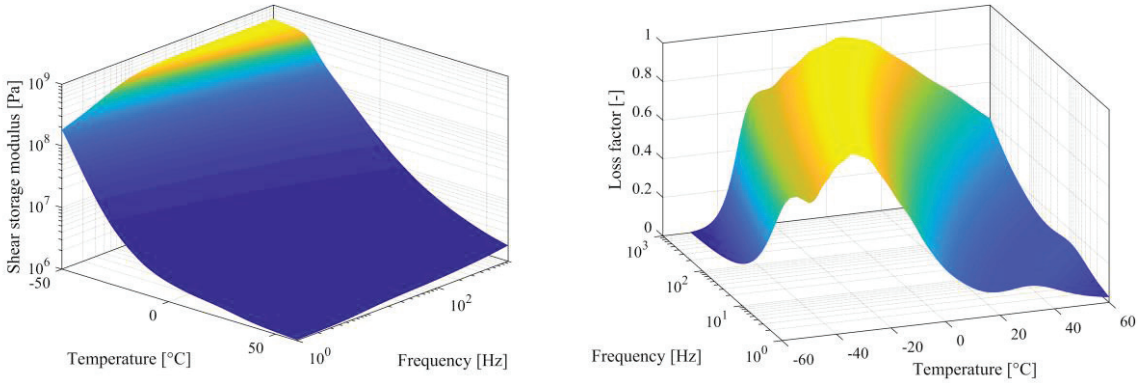

(a) (b)

Figure 4 – Shear storage modulus (a) and loss factor (b) of bromobutyl rubber

For the storage modulus a considerable decrease can be detected with increasing temperature - the material becomes more flexible. In addition, the material behaves stiffer for higher frequencies in isothermal consideration. In comparison, the contour curves of the loss factor are completely different. The area of maximum values extends slightly diagonally from low temperature (-40 °C) and low frequency (1 Hz) to higher frequencies at higher temperatures (1000 Hz at 0 °C). Outside this range, the loss factor drops considerably.

For the simulation, commercial FEM software Ansys 18 is used. The structure is discretized by PLANE182 elements, since this type of elements can map frequency- and temperature-dependent behavior. Because modal analysis with frequency- and temperature-dependent material properties cannot be carried out in the current software version, the beam is examined by means of a harmonic response analysis. Therefore, the beam is excited by a harmonic force with constant amplitude at a free end in vertical direction and the resulting frequency response functions (FRF's) are calculated for the excitation point. Edge effects due to thermal expansion are not taken into account in the analysis.

3.2 Damping performance of CLD treatment

The system described in the previous chapter is examined at five temperature levels. Using the peak-fit method (9), the modal parameters of the first three bending modes are identified from the resulting FRF's. The identified damping ratios are shown in Figure 5. For comparison purpose, the values given for the eigenfrequencies f_m correspond to the mean values of the respective mode from all temperature levels. However, the influence on the eigenfrequencies is not considered in the following. The dashed line in the diagram indicates the damping value of the undamped beam.

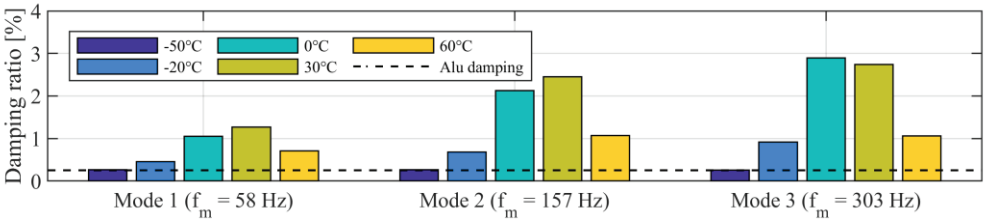

Figure 5 - Impact of frequency and temperature on damping capabilities of the CLD treatment

For the first and second mode, the order of damping ratios is identical. The highest damping ratios occur at a temperature of 30 °C. The second highest values appear at 0 °C, while the lowest damping ratios are recorded at lowest temperatures of -50 °C and -20 °C. However, the order of damping ratios changes for the third mode. In opposite to the first two modes, the damping value for 0 °C is highest at this point. In order to get a better understanding of the presented results, the contour curves of Figure 4 are plotted from top view in Figure 6. The horizontal lines indicate the particular eigenfrequencies, the vertical ones are isothermal lines.

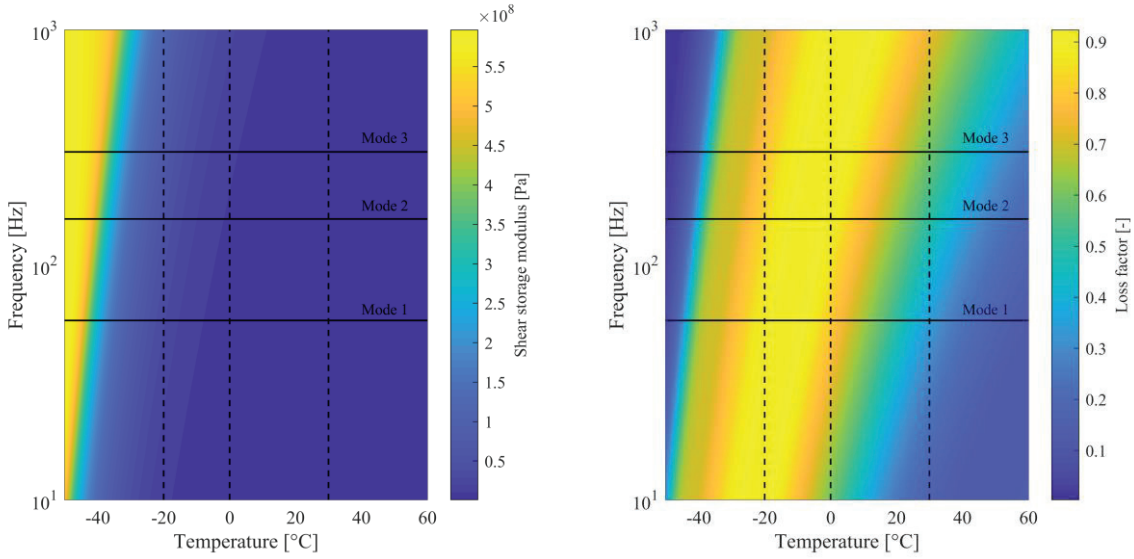

(a) (b)

Figure 6 – Top view on the contour curves of the shear storage modulus (a) and loss factor (b)

When considering the loss factor of the first mode in Figure 6(b), it is noticeable that the maximum damping ratio does not occur at the same temperature as the maximum loss factor of bromobutyl rubber. This also applies to other modes: Although the loss factor values for a temperature of -20 °C are above the values for 30 °C for all modes, the resulting damping ratio is always lower. From this fact it can be concluded that the loss factor is not the only decisive factor for damping, but also the stiffness of the material, represented by the shear storage modulus, is essential. Concerning that assumption, it is striking that the storage modulus is also lower for 30 °C than for -20 °C at all modes, as demonstrated in Figure 6(a). From that point it could be erroneously concluded, that low stiffness is appropriated in order to obtain high damping ratios.

The reason of the above mentioned behavior is founded in the prevailing damping mechanism. For CLD treatments, the damping mechanism is based on energy dissipation due to shear deformation. A quantity of the real potential energy W of elastic deformation is given by (10), regarding to a displacement vector $\boldsymbol{u}$:

$$W = \frac{1}{2}\boldsymbol{u}^T \boldsymbol{K} \boldsymbol{u} \tag{18}$$

If viscoelasticity is applied, the stiffness matrix becomes complex, as demonstrated in section 2.3. In a harmonic state of oscillation, excited by a force vector $\boldsymbol{f}$, the displacement vector becomes complex as well:

$$\boldsymbol{u}^* = [-\Omega^2 \boldsymbol{M} + \boldsymbol{K}^*(\Omega, T)]^{-1} \boldsymbol{f} \tag{19}$$

Here, $\boldsymbol{M}$ denotes the system mass matrix of the structure. Inserting Equation (19) into Equation (18) with a complex stiffness matrix $\boldsymbol{K}^*(\Omega, T)$ yields a scalar value of the complex energy W^*:

$$W^* = \frac{1}{2}[[-\Omega^2 \boldsymbol{M} + \boldsymbol{K}^*(\Omega, T)]^{-1} \boldsymbol{f}]^T \, \boldsymbol{K}^*(\Omega, T) \, [[-\Omega^2 \boldsymbol{M} + \boldsymbol{K}^*(\Omega, T)]^{-1} \boldsymbol{f}] \tag{20}$$

The real part of the potential energy is required for the calculation of the modal loss factor η_k, an indicator of the damping capability of a vibrating system (11):

$$\eta_k = \frac{\sum_{i=1}^{n} \eta_{i,k} W_{i,k}}{W_{total,k}} \tag{21}$$

$\eta_{i,k}$ is the loss factor and $W_{i,k}$ the modal strain energy of layer i at mode k, while $W_{total,k}$ denotes the total modal strain energy of the whole system at mode k. First, an essential perception can be derived from Equation (20), in which the complex stiffness matrix occurs in both an inverse and in an original form: Low stiffness leads to high energy dissipation due to high displacement. On the other hand, low stiffness of the viscoelastic layer causes a reduction of the modal loss factor, since the total energy in the denominator of Equation (21) increases. From that fact it can be derived, that an optimal composition of the stiffness matrix exists for each excitation frequency and temperature, which maximizes the dissipative energy and as a consequence, maximizes the damping ratio.

Relating to the above mentioned phenomena, the loss factor of -20 °C is considerably higher than for 30 °C, but it does not yield any advantage due to less shear deformation as a consequence of increased stiffness. In the case of the third mode, the combination of loss factor and shear storage modulus is more effective for 0 °C than for 30 °C.

3.3 Procedures for stiffness matrix modification

In order to maximize the damping performance, an optimal combination of stiffness matrix and material loss factor has to be found. The evolution of the material characteristics is given for a range of operating frequency and temperature. As shown in section 2.3, the stiffness matrix is determined from element shape functions and from the elasticity matrix. With given material, these cannot be used as design variables. However, the geometry of the finite elements provides another possibility to tailor the complex stiffness matrix for maximum damping. A geometry modification of a structure always involves a modification of the stiffness matrix. The thickness or the width of the viscoelastic layer is a possible design variable for the adjustment of the complex stiffness matrix. Of course, it is possible to use the spatial position of a local CLD treatment as a design variable. However, in this example, the CLD layer is modelled continuously so that this parameter cannot be used.

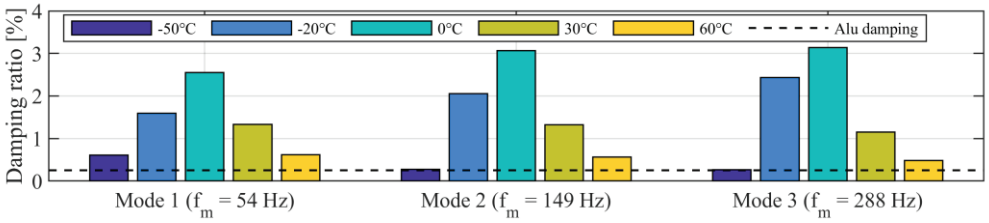

Figure 7 - Impact of frequency and temperature on damping capabilities of the cut CLD treatment

With the intention to create higher shear strain in the viscoelastic core layer, Lepoittevin et al. inserted small cuts into the core and face layer and examined the effects on damping (11). By this procedure, the stiffness matrix of the whole structure is modified. Hence, this approach is adopted here and applied on the beam from section 3.1 in the following. According to a rule of thumb (11), cuts at positions of maximum bending moment are most noticeable on damping. For this reason, the core and face layers are cut at position x=500 mm for the first mode, at positions x=310 mm and x=690 mm for

the second mode and at positions x=220 mm, x=500 mm and x=780 mm for the third mode with a gap of 1 mm each. The resulting damping ratios are shown in Figure 7.

First of all it is noticeable that the eigenfrequencies are lower than in the case of the continuous CLD treatment. This fact already indicates an overall stiffness decrement. However, the change of the eigenfrequencies is small compared to the conventional CLD treatment that it has a negligible influence on the material parameters of bromobutyl rubber. Furthermore, the maximum damping ratios occur in a different order compared to Figure 5. For all modes, the damping ratios for 0 °C are highest, followed by those of -20 °C and 30 °C. For lower temperatures, the cuts seem to have a positive effect, since an increase in the damping values can be observed. This confirms the assumption of inadequate stiffness in the case of continuous CLD treatment. In contrast, the effect of cuts is negative at higher temperatures. While the damping ratios are still at the same level as for the continuous CLD treatment for 30 °C and 60 °C at the first mode, the damping ratios even decrease for higher modes.

The instance of disadvantageous stiffness modification has to be considered during the design process as well. Otherwise, a mass increase due to damping material thickening, could even lead to the opposite of the pursued objective - a reduction of damping due to improper stiffness.

4. CONCLUSIONS

In this paper, the modelling of viscoelastic material in frequency domain by a generalized Maxwell model has been presented. By using Williams-Landel-Ferry and Arrhenius approaches, it was shown how the temperature dependence on the essential damping properties, storage modulus and loss factor, can be incorporated in the material model. Additionally, by using Hooke's law, the one-dimensional material model can be transformed into a multi-dimensional one. Due to the complex elasticity matrix, a complex stiffness matrix can be generated for FEM applications in which the imaginary part corresponds to a hysteretic damping matrix. As an example, the frequency and temperature dependent material behavior of a bromobutyl rubber mixture has been introduced and its effects on the damping performance of a CLD treatment have been analyzed for different frequency and temperature levels. On the one hand it has been shown that both frequency and temperature have a significant influence on the damping performance. On the other hand it has been demonstrated that a high loss factor does not necessarily lead to high damping ratios of a vibrating system, but especially the stiffness in terms of the storage modulus has to be considered. Only an appropriate combination of a high loss factor and a certain stiffness leads to maximum damping ratios.

REFERENCES

1. Vasques CMA, Moreira RAS, Dias Rodrigues J. Viscoelastic Damping Technologies–Part I: Modeling and Finite Element Implementation Journal of Advanced Research in Mechanical Engineering 2010;1(2):76-95.
2. Michaeli W, Brandt M, Brinkmann M, Schmachtenberg E. Simulation des nicht-linear viskoelastischen Werkstoffverhaltens von Kunststoffen mit dem 3D-Deformationsmodell. Zeitschrift für Kunststofftechnik. 2006;3(4).
3. Böswald M, Gröhlich M, Biedermann J, Winter R. Analysis and simulation of structures with local visco-elastic damping from elastomers. International Conference on Noise and Vibration Engineering (ISMA 2018); Leuven, Belgium2018.
4. Mottahedi M, Dadalau A, Hafla A, Verl A. Numerical analysis of relaxation test based on Prony series material model. Integrated Systems, Design and Technology 2010: Springer; 2011. p. 79-91.
5. Ansys Inc. Theory Reference for the Mechanical APDL and Mechanical Applications: Ansys Inc.; 2018.
6. Schwarzl FR. Polymermechanik: Struktur und mechanisches Verhalten von Polymeren: Springer-Verlag; 1990.
7. Scholz A. Ein Beitrag zur Optimierung des Schwingungsverhaltens komplexer Rotorsysteme mit viskoelastischen Dämpfungselementen [PhD]. Berlin: Technische Universität Berlin; 2011.
8. Link M. Finite Elemente in der Statik und Dynamik: Springer-Verlag; 2014.
9. Böswald M. Analysis of the bias in modal parameters obtained with frequency-domain rational fraction polynomial estimators. International Conference on Noise and Vibration Engineering (ISMA 2016); Leuven, Belgium2016.
10. Bathe K-J. Finite Element Procedures: Prentice Hall; 1996.
11. Lepoittevin G, Kress G. Optimization of segmented constrained layer damping with mathematical programming using strain energy analysis and modal data. Materials & Design. 2010;31(1):14-24.